Screening properties of a charged Bose condensate: bound states between equally charged particles

1999 J. Phys.: Condens. Matter 11 2379

(http://iopscience.iop.org/0953-8984/11/11/009)

J. Phys.: Condens. Matter **11** (1999) 2379–2393. Printed in the UK PII: S0953-8984(99)97817-7

Screening properties of a charged Bose condensate: bound states between equally charged particles

A Gold† and A Ghazali‡

† Centre d'Elaboration de Matériaux et d'Etudes Structurales (CEMES-CNRS), 29 Rue Jeanne Marvig, 31055 Toulouse, France

‡ Groupe de Physique des Solides, UMR 7588-CNRS, Universités Paris 7 et 6, 2 place Jussieu, 75251 Paris, France

Received 25 September 1998, in final form 9 December 1998

Abstract. We study the screening properties of three- and two-dimensional charged Bose condensates including many-body effects via a local-field correction. The screened test-charge–test-charge interaction, the test-charge–boson interaction and the boson–boson interaction for *equally charged* particles are calculated and found to be *attractive* at intermediate distances due to overscreening effects. Using the variational method and the matrix diagonalization method we determine the energies and wave functions of the ground state and excited states as functions of the Bose condensate density. For densities larger than a critical density no bound states are found. Below the critical density the number and the energy of bound states relative to the continuum increase and then saturate with decreasing Bose condensate density.

1. Introduction

Screening effects are essential in interacting quantum liquids. The screening properties of fermion systems have been discussed extensively in the literature and are described in many text books. The screening properties of Bose condensates are less known and only a few papers have considered such effects. In the following we discuss some consequences of screening provided by a charged Bose condensate especially the effect of screening on *equally* charged particles.

Recently, it has been shown that two equally charged test-particles imbedded in an electron gas with a low enough density can have bound states when the screening supplied by the medium is taken into account. This was shown for interacting electron systems in one [1], two [2, 3] and three [3, 4] dimensions. One might believe that the presence of Friedel oscillations [5] in electron systems is the origin of this attraction. In the present paper we show that attraction between equally charged particles also occurs when the test-particles are screened by a Bose condensate. Already within the random-phase approximation (RPA) it can be shown that the screened potential within a Fermi or Bose gas has an attractive part at any density, but bound states only exist in *low* density systems. The attractive part in the screened potential is an overscreening effect, which is a strong effect when the screening is due to a Bose condensate.

A necessary but not sufficient condition for supraconductivity is the attraction between *equally* charged particles. This attraction can be called *overscreening* and is in general a retarded interaction [6]. The present model of overscreening effects in a Bose condensate shows that attraction for a non-retarded interaction due to overscreening can occur.

0953-8984/99/112379+15$19.50

We have a few reasons to motivate our study of a Bose condensate. (i) A three-dimensional charged Bose condensate is expected to be an important model system for astrophysical applications [7] and it is interesting to study the screening properties of such a condensate. (ii) A two-dimensional Bose condensate can be considered as a model for high-T_c superconductors. In high-T_c superconductors paired electrons are tightly bound together and a Bose condensate of such pairs might be a simple model to describe some properties of these systems [8, 9]. (iii) The recent discovery of Bose condensation of neutral sodium atoms and the study of elementary excitations [10] will certainly lead to more interest in properties of boson systems. (iv) Finally, a Bose condensate is an elementary but non-trivial system in statistical mechanics and the attraction between equally charged particles, due to screening by a Bose condensate, is certainly of interest from a theoretical point of view.

The existence of an attractive part in the interaction potential between equally charged particles in the case of screening by a Bose condensate is well known in three dimensions (3D) [11] and two dimensions (2D) [12]. However, bound state energies have never been calculated. We show that many-body effects, described by the local-field correction, increase the attraction as compared with that of the RPA.

Many-body effects have been discussed in recent years for the 3D charged Bose condensate [13–18] and for the 2D charged Bose condensate [18–20]. The many-body effects are described by a function $G(q)$, called the local-field correction (LFC). For a review, see [21]. The LFC is essential in order to describe the interaction potential in the low density domain [22], in contrast to the high density limit where the RPA is exact and the LFC can be neglected.

In section 2 we describe the model and the theory. Our results for bound states between equally charged particles induced by screening effects due to the Bose condensate in 3D are described in section 3. The results for a 2D Bose condensate are given in section 4. The screened boson–boson interaction is discussed in section 5. A discussion of our results is given in section 6. The conclusion is found in section 7.

2. Model and theory

2.1. Model: the screened Coulomb interaction

As the model we use a d-dimensional Bose gas ($d = 3, 2$) with a parabolic dispersion and density N_d. Distances are given in units of the effective Bohr radius $a^* = \varepsilon_L/m^*e^2$ with the Planck constant $h/2\pi = 1$. Wave numbers are given in units of the inverse Bohr radius. m^* is the effective mass and ε_L is the dielectric constant of the background. Energy values are expressed in units of the effective Rydberg $\mathrm{Ry}^* = m^*e^4/2\varepsilon_L^2$. The density parameter (or Wigner–Seitz parameter) r_s is given by $r_s = [3/4\pi N_3 a^{*3}]^{1/3}$ for 3D and by $r_s = [1/\pi N_2 a^{*2}]^{1/2}$ for 2D.

The model we consider is a jellium model for a Bose condensate: if the Bose condensate is negatively charged there is a positive background charge to ensure charge neutrality. The interaction potential between the bosons is denoted by $V(q)$ in the Fourier space. The bare (b) Coulomb interaction potential between two equally charged particles is repulsive and given by $V_b(q) = +V(q)$ with $V(q) = 4\pi e^2/\varepsilon_L q^2$ in 3D and $V(q) = 2\pi e^2/\varepsilon_L q$ in 2D. Here and in the following, a Bose particle is assumed to hold a single elementary charge. However, our results can be rescaled according to the effective charge and mass of bosons under consideration.

The screened test-charge–test-charge (tt) interaction $V_{tt,sc}(q)$ is given in terms of the screening function $\varepsilon_{tt}(q)$ by

$$V_{tt,sc}(q) = \frac{V_b(q)}{\varepsilon_{tt}(q)}. \tag{1}$$

We assume the two *test-charges* to be distinct from the boson medium providing the screening. The dielectric function $\varepsilon_{tt}(q)$ is given by $1/\varepsilon_{tt}(q) = [1 - V(q)G(q)X_0(q)]/[1 + V(q)[1 - G(q)]X_0(q)]$ and $G(q)$ is the LFC function. $X_0(q) = 4N_d m^*/q^2$ is the static density–density response function of the free Bose condensate [11, 12, 14]. In fact, the form for $1/\varepsilon_{tt}(q)$ as given above was derived for electron screening [22], but the same reasoning holds for Bose condensate screening. However, as will be seen below, the screening properties of charged Bose and electron systems differ in many respects due to different response functions $X_0(q)$.

In the following $G_2(q)$ and $G_3(q)$ denote the LFC functions in 2D and 3D, respectively. For 3D the dielectric function for the test-charge–test-charge interaction is given by

$$\frac{1}{\varepsilon_{tt}(q)} = 1 - \frac{1}{1 - G_3(q) + q^4/q_3^4} \tag{2a}$$

with $q_3 a^* = 12^{1/4}/r_s^{3/4}$. $1/q_3$ is the relevant length scale for screening in the 3D Bose condensate and goes to infinity for $r_s \to \infty$, which corresponds to the unscreened limit. The dielectric function in 2D is expressed as

$$\frac{1}{\varepsilon_{tt}(q)} = 1 - \frac{1}{1 - G_2(q) + q^3/q_2^3} \tag{2b}$$

with $q_2 a^* = 2/r_s^{2/3}$. Here $1/q_2$ is the relevant length scale for screening.

The screened test-charge–boson (tb) interaction $V_{tb,sc}(q)$ is written as

$$V_{tb,sc}(q) = \frac{V_b(q)}{\varepsilon_{tb}(q)} \tag{3}$$

where the inverse dielectric function for tb interaction is $1/\varepsilon_{tb}(q) = 1/[1 + V(q)[1 - G(q)]X_0(q)]$ [22]. This leads in 3D to

$$\frac{1}{\varepsilon_{tb}(q)} = 1 - \frac{1 - G_3(q)}{1 - G_3(q) + q^4/q_3^4} \tag{4a}$$

and in 2D to

$$\frac{1}{\varepsilon_{tb}(q)} = 1 - \frac{1 - G_2(q)}{1 - G_2(q) + q^3/q_2^3}. \tag{4b}$$

For $G(q) = 0$ one obtains the familiar RPA expression:

$$\varepsilon_{RPA}(q) = 1 + V(q)X_0(q) \tag{5}$$

with $V_{RPA}(q) = V_b(q)/\varepsilon_{RPA}(q)$. For $r_s \ll 1$ the LFC can be neglected and one obtains $\varepsilon_{tt}(q) \approx \varepsilon_{tb}(q) \approx \varepsilon_{RPA}(q)$. However, for $r_s > 1$ one must carefully discriminate which kind of interaction one wants to study. $\varepsilon_{tb}(q)$ takes a different form from $\varepsilon_{tt}(q)$ to account for the indistinguishability of bosons.

In our calculation we use for the LFC the sum-rule approximation [18] of the Singwi–Tosi–Land–Sjölander (STLS) approach. For a review on the STLS approach, see [23]. The LFC is parametrized by three coefficients $C_{id}(r_s)$ $(i = 1, 2, 3)$. For the 3D Bose condensate the LFC function is written as

$$G_3(q) = r_s^{3/4} \frac{0.846q^2}{2.188q_3^2 C_{13}(r_s) + q^2 C_{23}(r_s) - q_3 q C_{33}(r_s)} \tag{6a}$$

and for the 2D Bose condensate as

$$G_2(q) = r_s^{2/3} \frac{1.402q}{[2.644q_2^2 C_{12}(r_s)^2 + q^2 C_{22}(r_s)^2 - q_2 q C_{32}(r_s)]^{1/2}}. \tag{6b}$$

The coefficients are determined in the same way as for electrons [24]. $C_{1d}(r_s)$ is determined from the compressibility of the condensate calculated within the STLS approach. In the STLS

description, the pair correlation function $g(r = 0)$ is connected with the LFC function for large wave numbers via $G(q \to \infty) = 1 - g(r = 0)$: this defines $C_{2d}(r_s)$. The coefficient $C_{3d}(r_s)$ is calculated using the relation between the pair-correlation function $g(r = 0)$ and the static structure factor $S(q)$. Therefore the LFC fulfils the compressibility sum rule. Details will be published elsewhere [25].

2.2. Bound states

The Schrödinger equation for the screened potential is solved numerically in the momentum space. This equation reads

$$\frac{q^2}{2m^*}\psi(\boldsymbol{q}) + \frac{1}{(2\pi)^d}\int \mathrm{d}^d\boldsymbol{q}' V_{sc}(\boldsymbol{q}-\boldsymbol{q}')\psi(\boldsymbol{q}') = E\psi(\boldsymbol{q}). \tag{7}$$

Equation (7) has been discretized according to $\boldsymbol{q}$ and $\boldsymbol{q}'$ to give a matrix equation. V_{sc} in equation (7) represents V_{RPA}, $V_{tb,sc}$ or $V_{tt,sc}$. The eigenenergy and eigenfunction problem is then solved numerically by a standard method for matrix diagonalization. Details can be found in [4].

For 3D the wave function $\psi(\boldsymbol{r})$ is given by $\phi_{n_r l}(r)Y_{lm}(\varphi,\theta)$. The degeneracy of the eigenstates is $g_l = 2l + 1$. $\phi_{n_r l}(r)$ is the solution of the radial Schrödinger equation for the effective potential $V_{eff}(r) = V_l(r) + V_{sc}(r)$ with $V_l(r) = l(l+1)/2m^*r^2$.

For 2D the wave function is given by $\psi(\boldsymbol{r}) = \phi_{n_r l}(r)\exp[\pm \mathrm{i}l\varphi]$ with degeneracy $g_l = 1$ for $l = 0$ and $g_l = 2$ for $l > 0$. $\phi_{n_r l}(r)$ is the radial wave function for the effective potential $V_{eff}(r) = V_l(r) + V_{sc}(r)$ with $V_l(r) = l^2/2m^*r^2$. In the momentum space the wave function is written as $\psi(\boldsymbol{q}) = \phi_{n_r l}(q)\exp(\pm \mathrm{i}l\varphi)$. In the following $\phi(r)$ is used instead of $\phi_{n_r l}(r)$.

Using a trial wave function $\phi_{var}(r)$ the variational (var) energy is given by $E_{var} = \langle T\rangle + \langle V_l\rangle + \langle V_{sc}\rangle$. The average $\langle O\rangle$ means $\langle O\rangle = \int_0^\infty \mathrm{d}r r^{d-1}\phi_{var}(r)O\phi_{var}(r)$. For certain simple wave functions the r-integrals for $O = T$, V_l and V_{sc} can be calculated analytically. The shape of the effective potential leads us to choose a variational radial wave function containing a Gaussian factor:

$$\phi_{var}(r) = Ar^{k_1/2}\exp(-r^2/2\alpha^2) \tag{8}$$

with the normalization constant A and the variational parameters k_1 and α. The explicit expressions for $\langle T\rangle$, $\langle V_l\rangle$ and $\langle V_{sc}\rangle$, depending on the screening function, can be found in our earlier work on electron screening [2–4].

The variational wave function $\phi_{var}(r)$ shows a maximum at $r^* = (k_1/2)^{1/2}\alpha$. For $k_1 > 0$ the wave function has a node at $r = 0$ and corresponds to $n_r = 1$. For different values of l the notation of the state $n_r l$ is 1s, 1p and 1d for $l = 0, 1, 2$, respectively. The bound states are very extended in space due to the large Coulomb repulsion at small distances.

In the following we present results for bound states within the RPA and the tb and the tt interaction. In general we only find bound states for $r_s > 1$ (or $r_s \gg 1$), where the RPA is no longer applicable. The results within the RPA are given for comparison with the results obtained for the tb and the tt interaction: the importance of many-body effects described by the LFC is thus demonstrated.

3. Results for three dimensions

3.1. The screened potential

In the real space the screened Coulomb interaction in 3D is given by

$$V_{sc}(r) = \frac{1}{2\pi^2 r}\int_0^\infty \mathrm{d}q\, q\sin(qr)V_{sc}(q). \tag{9}$$

Within the RPA $V_{sc}(r)$ can be calculated analytically:

$$V_{RPA}(r)/\mathrm{Ry}^* = 2\frac{a^*}{r}\exp(-rq_3/2^{1/2})\cos(rq_3/2^{1/2}). \tag{10}$$

This potential has a minimum at

$$r_{min}/a^* = 1.650 r_s^{3/4} \tag{11a}$$

with an attractive part

$$V_{RPA}(r_{min})/\mathrm{Ry}^* = -0.0781/r_s^{3/4}. \tag{11b}$$

$V_{RPA}(r_{min})r_{min} = -0.1288$ Ry* a^* is independent of r_s. We also note that V_{RPA} is zero for $r_1/a^* = 1.193 r_s^{3/4}$ and $r_2/a^* = 3.581 r_s^{3/4}$ with $r_1 < r_{min} < r_2$. This shows that already within the RPA an attractive region ($r_1 < r < r_2$) in the screened potential exists and $|V_{RPA}(r_{min})| \propto 1/r_s^{3/4}$ *increases* with *decreasing* r_s. The attractive part in the screened potential is an overscreening effect. At this point it is obvious to ask whether are there bound states. However, to our knowledge, this question was never asked in the literature.

A representative example for $V_{sc}(r)$ versus r is shown in figure 1. For $r_s = 1$ we find a minimum $V_{tt,sc}(r_{min}) = -0.108$ Ry* at $r_{min} = 1.55\ a^*$. Note the strong Coulomb repulsion for small distances. For $r_s = 1$ the differences between $V_{RPA}(r)$, $V_{tb,sc}(r)$ and $V_{tt,sc}(r)$ are already visible.

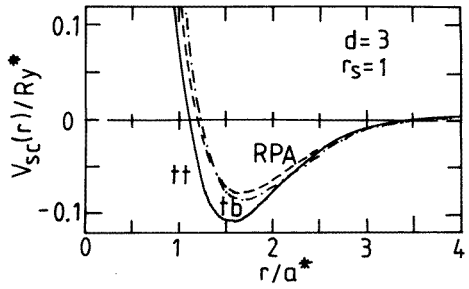

Figure 1. Screened potential $V_{sc}(r)$ versus distance r for $r_s = 1$ in 3D for equally charged particles. The solid (dashed–dotted) line represents the test-charge–test-charge (tt) (test-charge–boson (tb)) interaction. The dashed line represents the RPA.

A systematic study of r_{min} and $V_{sc}(r_{min})$ versus r_s for the RPA, and with the LFC for the tb and tt interactions is shown in figure 2. For large r_s we note that the attractive part for the tt interaction is strongly increased. For $r_s > 3$ we find $V_{tt,sc}(r_{min}) \approx -0.07$ Ry*. Of course, the results shown in figure 2 present limits for the bound state energies. While the difference between the RPA and the tb interaction seems to be small, we will see that the respective bound state energies are quite different.

3.2. Bound states

In the RPA our results for the binding energy versus r_s are shown in figure 3. The binding energies are of the order of 0.4 mRy*. From the matrix diagonalization calculation we conclude: for $r_s < r_{sc} = 23$ no bound state exists and in the range $23 < r_s < 80$ we found a single bound state. Our variational model gives a slightly smaller binding energy than the exact matrix diagonalization method. The state 1p is threefold degenerate. The binding energies within the RPA are quite small and the ground state is very extended ($\alpha \approx 40\ a^*$).

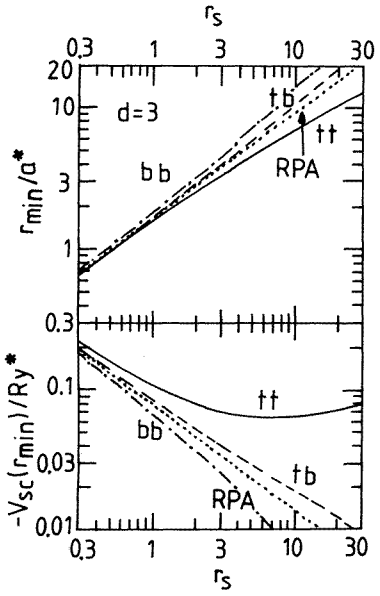

Figure 2. r_{min} and $V_{sc}(r_{min})$ versus r_s for 3D and equally charged particles. The solid (dashed) lines represent the test-charge–test-charge (tt) (test-charge–boson (tb)) interaction. The dotted lines represent the RPA according to equation (11). The dashed–dotted lines represent the boson–boson (bb) interaction.

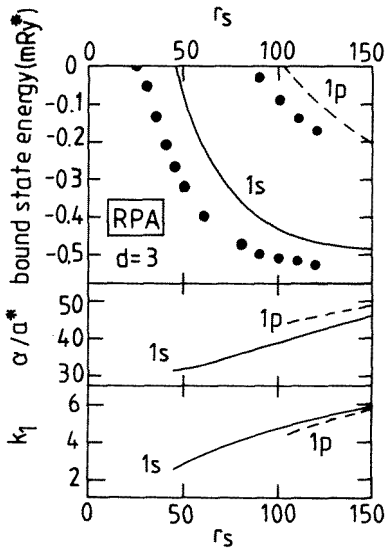

Figure 3. Binding energy for equally charged particles and variational parameters α and k_1 versus r_s for $n_r = 1$ and $l = 0, 1$ in 3D within the RPA. The solid dots are obtained by matrix diagonalization.

Let us discuss some numbers for $r_s = 100$. The attractive part of the screened potential is already small: $V_{RPA}(r_{min}) = -2.5$ mRy*. We note that the 1s state has a binding energy of -0.5 mRy*. For the maximum of the wave function we obtain $r^* = 57.1\ a^*$ while the minimum of the screened potential is located at $r_{min} = 52.2\ a^*$.

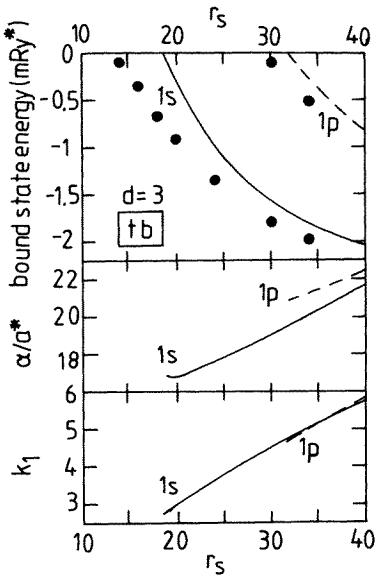

Figure 4. Binding energy for equally charged particles and variational parameters α and k_1 versus r_s for $n_r = 1$ and $l = 0, 1$ in 3D for the test-charge–boson (tb) interaction. The solid dots are obtained by matrix diagonalization.

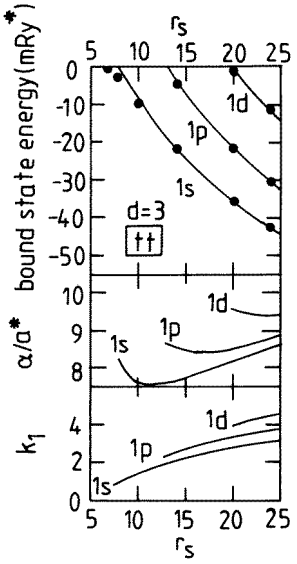

Figure 5. Binding energy for equally charged particles and variational parameters α and k_1 versus r_s for $n_r = 1$ and $l = 0, 1, 2$ in 3D for the test-charge–test-charge (tt) interaction. The solid dots are obtained by matrix diagonalization.

For the tb interaction the results for the binding energy versus r_s are shown in figure 4. The binding energies are of the order of 1.5 mRy*, a factor of three larger than within the RPA. For $r_s < r_{sc} = 13$ no bound state exists and the ground state is less extended ($\alpha \approx 20\, a^*$) than within the RPA.

For the tt interaction the results for the binding energy versus r_s are shown in figure 5. The binding energies are of the order of 40 mRy*, a factor of 100 larger than within the RPA. For $r_s < r_{sc} = 6.5$ no bound state exists and the ground state is much less extended ($\alpha \approx 8\,a^*$) than within the RPA.

4. Results for two dimensions

4.1. The screened potential

In 2D the screened Coulomb interaction in the real space is given by

$$V_{sc}(r) = \frac{1}{2\pi}\int_0^\infty \mathrm{d}q\, q\, J_0(rq) V_{sc}(q). \tag{12}$$

$J_0(x)$ is the zero-order Bessel function of the first kind.

Within the RPA the screened potential is given by

$$V_{RPA}(r)/\mathrm{Ry}^* = \frac{a^*}{r} - 2q_2 a^* \int_0^\infty \mathrm{d}y\, J_0(yrq_2)/(1+y^3). \tag{13}$$

The integral can be calculated analytically and expressed in terms of Bessel and Struve functions. One can show that $V_{RPA}(r)$ has a minimum at

$$r_{min}/a^* = 0.956 r_s^{2/3} \tag{14a}$$

with

$$V_{RPA}(r_{min})/\mathrm{Ry}^* = -0.384/r_s^{2/3} \tag{14b}$$

and $V_{RPA}(r_{min})r_{min} = -0.367$ Ry* a^* is independent of r_s. V_{RPA} vanishes for $r_1/a^* = 0.586 r_s^{2/3}$ and $r_2/a^* = 3.302 r_s^{2/3}$ with $r_1 < r_{min} < r_2$. Thus, within the RPA an attractive part ($r_1 < r < r_2$) exists and $|V_{RPA}(r_{min})| \propto 1/r_s^{2/3}$ *increases* with *decreasing* r_s.

A representative example for $V_{sc}(r)$ versus r is shown in figure 6 for $r_s = 1$ with a minimum of $V_{tt,sc}(r_{min}) = -0.69$ Ry* at $r_{min} = 0.83a^*$. Again, we conclude that many-body effects described by the LFC are already very important for $r_s = 1$.

r_{min} and $V_{sc}(r_{min})$ versus r_s are shown in figure 7. In 2D $V_{tt,sc}(r_{min})$ for $r_s = 10$ is a factor of ten larger than in 3D. For $r_s > 2$ we find $V_{tt,sc}(r_{min}) \approx -0.6$ Ry*. Again we note that for $r_s > 1$ the differences between the RPA and the tb interaction are small, compared with the differences between the RPA and the tt interaction.

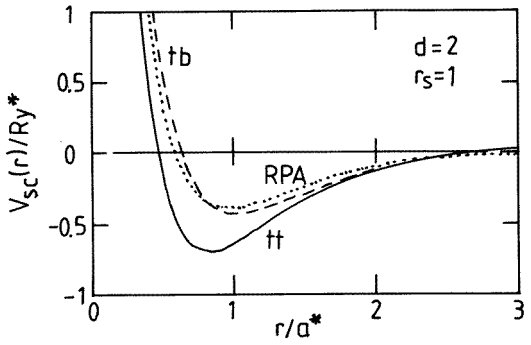

Figure 6. Screened potential $V_{sc}(r)$ versus distance r for $r_s = 1$ in 2D for equally charged particles. The solid (dashed) line represents the test-charge–test-charge (tt) (test-charge–boson (tb)) interaction. The dotted line represents the RPA.

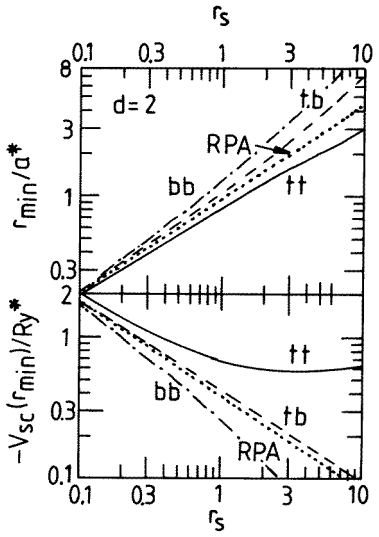

Figure 7. r_{min} and $V_{sc}(r_{min})$ versus r_s for 2D and equally charged particles. The solid (dashed) lines represent the test-charge–test-charge (tt) (test-charge–boson (tb)) interaction. The dotted lines represent the RPA according to equation (14). The dashed–dotted lines represent the boson–boson (bb) interaction.

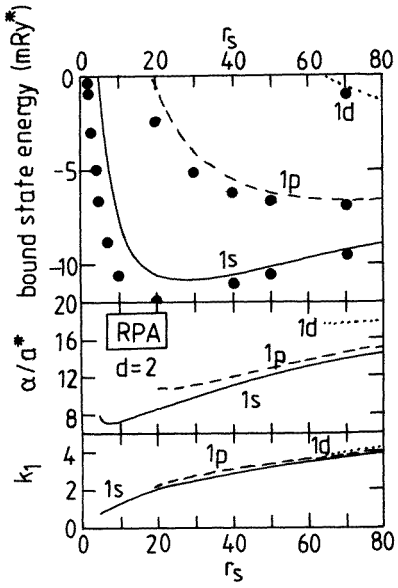

Figure 8. Binding energy for equally charged particles and variational parameters α and k_1 versus r_s for $n_r = 1$ and $l = 0, 1, 2$ in 2D within the RPA. The solid dots are obtained by matrix diagonalization.

4.2. Bound states

Within the RPA our results for the binding energy versus r_s are shown in figure 8. The binding energies are of the order of 8 mRy*. From the matrix diagonalization calculation we found:

for $r_s < r_{sc} = 1$ no bound state exists and for $1 < r_s < 10$ a single bound state is found. Our variational results give a slightly smaller binding energy than the exact matrix diagonalization. As in 3D we denote the states by two quantum numbers: the radial quantum number n_r and the angular quantum number l. The state 1p has a twofold degeneracy.

In 2D the ground state is less extended ($\alpha \approx 10\,a^*$) than in 3D. For $r_s = 20$ we obtain within the RPA the following numbers: $V_{RPA}(r_{min}) \approx -52$ mRy*, binding energy -10.7 mRy*, $r_{min} = 7.04\,a^*$ and $r^* = 8.9\,a^*$.

For the tb interaction the results for the binding energy versus r_s are shown in figure 9. The binding energies for the 1s state are of the order of 25 mRy*, a factor of three larger than within the RPA. For $r_s < r_{sc} = 0.7$ no bound state exists and the ground state is less extended ($\alpha \approx 6\,a^*$) than within the RPA.

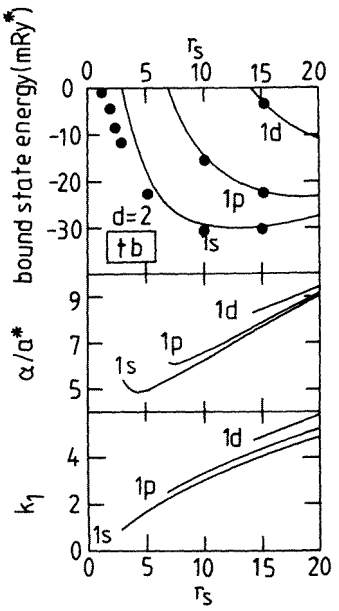

Figure 9. Binding energy for equally charged particles and variational parameters α and k_1 versus r_s for $n_r = 1$ and $l = 0, 1, 2$ in 2D for the test-charge–boson (tb) interaction. The solid dots are obtained by matrix diagonalization.

For the tt interaction the results for the binding energy versus r_s are shown in figure 10. The binding energies are of the order of 300 mRy*, a factor of 40 larger than within the RPA. For $r_s < r_{sc} = 0.5$ no bound state exists and the ground state is much less extended ($\alpha \approx 3\,a^*$) than within the RPA.

5. Screened boson–boson interaction

In this section we describe the effective interaction between two bosons screened by a Bose condensate. The two repulsive charges are now indistinguishable from other bosons which screen. The screened boson–boson (bb) interaction $V_{bb,sc}(q)$ is given by

$$V_{bb,sc}(q) = \frac{V_b(q)}{\varepsilon_{bb}(q)}. \tag{15}$$

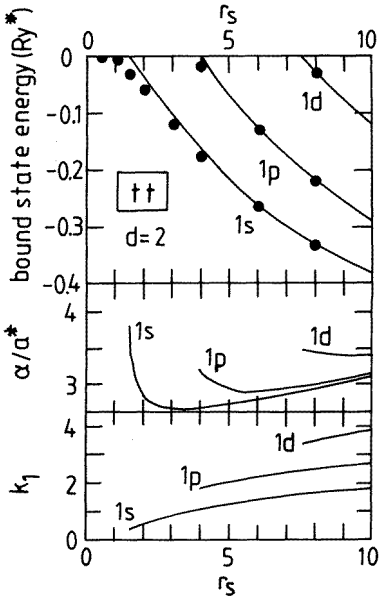

Figure 10. Binding energy for equally charged particles and variational parameters α and k_1 versus r_s for $n_r = 1$ and $l = 0, 1, 2$ in 2D for the test-charge–test-charge (tt) interaction. The solid dots are obtained by matrix diagonalization.

The inverse dielectric function for the bb interaction is given by $1/\varepsilon_{bb}(q) = [1 + V(q)[1 - G(q)]G(q)X_0(q)]/[1 + V(q)[1 - G(q)]X_0(q)]$. This result is obtained using the arguments given in [22] for electrons. In an electron system two different LFCs are needed to account for the spin. In a boson system one LFC describes all many-body effects.

Explicitly we find in 3D

$$\frac{1}{\varepsilon_{bb}(q)} = 1 - \frac{[1 - G_3(q)]^2}{1 - G_3(q) + q^4/q_3^4} \tag{16a}$$

and in 2D

$$\frac{1}{\varepsilon_{bb}(q)} = 1 - \frac{[1 - G_2(q)]^2}{1 - G_2(q) + q^3/q_2^3}. \tag{16b}$$

Note that $1/\varepsilon_{bb}(q)$ is similar to $1/\varepsilon_{tt}(q)$: replacing one test-charge by one boson introduces a factor $[1 - G(q)]$ in the second term on the r.h.s. of equation (2). The second term on the r.h.s. of equations (2) and (16) is nothing else than the screening term.

$V_{bb,sc}(r_{min})$ and r_{min} versus r_s are shown in figure 2 for three dimensions and in figure 7 for two dimensions. For large r_s we find $|V_{bb,sc}(r_{min})| \ll |V_{RPA}(r_{min})| < |V_{bt,sc}(r_{min})| \ll |V_{tt,sc}(r_{min})|$. This means that the binding energy for the boson–boson interaction, if any, should be much smaller than the RPA binding energy. For 2D an example of $V_{bb,sc}(r)$ is shown in figure 11 for $r_s = 15$.

We have searched for bound states of $V_{bb,sc}(r)$. In the 3D Bose condensate the bound state energies are very small, of order 6×10^{-6} Ry*. They are found for large r_s, $r_s \gg r_{sc} = 50$; see table 1. However, bound states with such a small binding energy at such low density probably disappear if a more accurate LFC is used.

In the 2D Bose condensate the bound state energies are of order 5×10^{-4} Ry* for $r_s \gg r_{sc} = 3$, see table 1. For $r_s = 15$ the ground-state wave function in the real space,

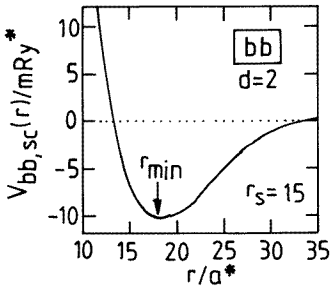

Figure 11. Screened potential $V_{bb,sc}(r)$ versus distance r for $r_s = 15$ in 2D for equally charged bosons.

Table 1. Critical Wigner–Seitz parameter r_{sc} for the appearance of the 1s state found by the matrix diagonalization method for 2D and 3D. The values in curly brackets are our results for r_{sc} found with the variational method. Ground state binding energies for $r_s \approx 3r_{sc}$ are denoted by $E_{1s}(3r_{sc})$ and are given to show the order of magnitude.

	$d = 3$		$d = 2$	
	r_{sc}	$E_{1s}(3r_{sc})$ (mRy*)	r_{sc}	E_{1s} $(3r_{sc})$ (mRy*)
boson–boson (bb)	50 {—}	-6×10^{-3}	3.0 {21.5}	-0.4
RPA	23 {46}	-0.4	0.9 {4.7}	-5
test–boson (tb)	13 {19}	-2	0.7 {2.9}	-10
test–test (tt)	6.5 {8}	-30	0.5 {1.5}	-100

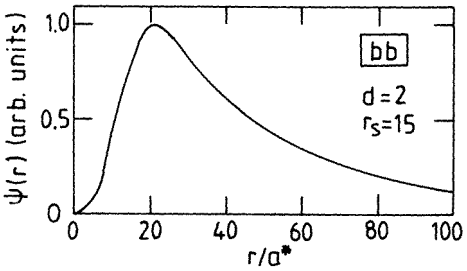

Figure 12. Wave function of the ground state versus distance r for $r_s = 15$ in 2D for equally charged bosons.

found with the diagonalization method, is shown in figure 12. It is very extended because $|E_{1s}/V_{bb,sc}(r_{min})| = 4.4\%$ only. For other r_s-values this ratio is also very small. Therefore, the variational method is no longer valid here; see our values for r_{sc} in table 1.

For the bb interaction, the results of the binding energy, obtained by the matrix diagonalization method, versus r_s are shown in figure 13 for 2D. We conclude that in 2D overscreening effects are important for the screened boson–boson interaction and they are strong enough to produce bound states of energy 0.5 mRy*. This could lead to an instability of the Bose condensate in 2D.

An important practical conclusion of our calculation concerning the bb interaction is the following. If many-body effects are taken into account, the bb interaction is much more like the RPA than the tt interaction or the tb interaction. In other words, in order to describe the bb interaction it is better to use the RPA than to use the tt interaction or the tb interaction.

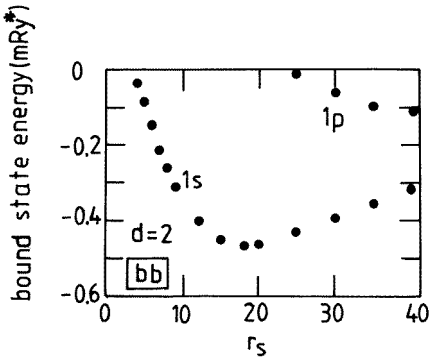

Figure 13. Binding energy versus r_s for the boson–boson (bb) interaction in 2D obtained by matrix diagonalization.

6. Discussion

In connection with high-T_c supraconductivity is was argued that the attraction between the electrons could be mediated by the Coulomb interaction which is assumed to be retarded via a dynamic process. In previous papers, we have shown that an attraction does occur between equally charged particles when a static screening is provided by an electron gas [1–4]. The present results for bound states between equally charged particles, due to static screening effects of a Bose condensate, extend the effect of overscreening to bosons and show that attraction between equally charged particles is a quite general phenomenon in charged quantum many-body systems. We think that these effects of static overscreening have not really been understood in the community and our calculation using screening by a Bose condensate might help us to be better prepared for such a kind of 'strange' attraction.

Our formulas for the 'effective' inverse static dielectric function also hold for the 'effective' inverse dynamic dielectric function by replacing $X_0(q)$ by $X_0(q, \omega)$.

The analytical results for r_{min} and $V_{RPA}(r_{min})$ within the RPA are interesting. For instance, it is generally believed that a bound state always exists in 2D if the potential is attractive. However, this statement is only true for a short-range potential. For screening by a Bose condensate within the RPA in 2D, no bound state exists for high density, in spite of a large value of $V_{RPA}(r_{min})/\mathrm{Ry}^* = -0.384/r_s^{2/3}$ in that case. This shows that a long-range potential give rise to unexpected results.

The matrix diagonalization method allows to determine the wave function of the ground state and of the excited states. From the study of the electron gas [2–4] we know that the variational method is a good approximation to the exact wave function; therefore we do not show explicit results in the case of screening by a Bose condensate. In the present paper we only give the variational results for the $n_r = 1$ states. We have also studied the $n_r = 2$ excited states; for the variational wave function, see [4]. But in general the binding energies of these states are much smaller than the binding energies of the 1s and the 1p states. Therefore, we do not give results for these states. We mention that the method used in [4] for $n_r = 2$ can also be applied to the system with a Bose condensate screening.

The general features found for the bound states in the case of screening by a Bose condensate are similar to those obtained for screening by an electron gas [2–4]. By reducing the dimension from three to two we find an increase of the binding energy by a factor of about 10. It is evident from these results that overscreening phenomena might be quite important in low

dimensional systems. Our results for r_{sc} and the binding energy of the 1s state are summarized in table 1. The exact diagonalization method gives values for r_{sc} which are substantially lower than the values obtained with the variational approach. This is an important result which shows that the diagonalization method is necessary for the determination of r_{sc}.

The critical value r_{sc}, where the binding energy of the 1s state disappears, is lower in the Bose condensate than in a system with fermion screening: compare our table 1 with table 1 in [3]. Our numerical results for the bb interaction indicates, see table 1, that there are no bound states in 3D, but in 2D bound states might exist. This could give rise to an instability of a Bose condensate in 2D.

We used in this paper the linear screening approximation. Our approach is similar to the widely used linear analysis of instability in non-linear problems. Indeed, in our paper we seek for the instability threshold in a homogenous gas with respect to many-body perturbations. In this sense, our approach is certainly correct. We believe that for repulsive charges non-linear screening effects are small because the wave functions are very extended, compared to the effective Bohr radius, and the binding energies are small, compared to the effective Rydberg. For attractive charges non-linear screening effects *might* be more important [26].

7. Conclusion

We have studied the screening by a charged Bose gas in 3D and 2D. The screened test-charge–test-charge, the test-charge–boson and the boson–boson interaction are investigated by using a screening function where many-body effects are included through the local-field correction. Bound states are found for the boson–boson interaction, the test-charge–boson and the test-charge–test-charge interaction in the low density range. The binding energy increases when the dimension of the system decreases and are strongly enhanced as compared to the corresponding values found within the RPA.

Our calculations show that the *attraction between equally charged particles*, induced by screening due to a charged Bose condensate, is an *overscreening* effect. This attraction seems to be a general property of many-particle systems. The overscreening effects become larger in low dimensional systems.

References

[1] Calmels L and Gold A 1995 *Phys. Rev.* B **51** 11 622
Calmels L and Gold A 1997 *Phys. Rev.* B **56** 1762
[2] Ghazali A and Gold A 1995 *Phys. Rev.* B **52** 16 634
Gold A and Ghazali A 1997 *J. Phys.: Condens. Matter* **9** 6885
[3] Gold A and Ghazali A 1997 *J. Phys.: Condens. Matter* **9** 3749
[4] Gold A and Ghazali A 1996 *J. Phys.: Condens. Matter* **8** 7393
[5] Friedel J 1953 *Adv. Phys.* **3** 446
[6] Waldram J R 1996 *Superconductivity of Metals and Alloys* (Bristol: Institute of Physics)
[7] Jetzer P 1992 *Phys. Rep.* **220** 163
[8] Gold A 1992 *Physica* C **190** 483
[9] Alexandrov A S and Mott N F 1993 *Supercond. Sci. Technol.* **6** 215
[10] Mewes M O, Andrews M R, van Druten N J, Kurn D M, Durfee D S, Townsend C G and Ketterle W 1996 *Phys. Rev. Lett.* **77** 988
[11] Lee J C 1975 *Phys. Rev.* B **12** 2644
[12] Hore S R and Frankel N E 1975 *Phys. Rev.* B **12** 2619
[13] Hansen J P and Mazighi 1978 *Phys. Rev.* A **18** 1282
[14] Caparica A A and Hipolito O 1982 *Phys. Rev.* A **26** 2832
[15] Sugiyama G, Bowen C and Alder B J 1992 *Phys. Rev.* B **46** 13 042
[16] Conti S, Chiofalo M L and Tosi M P 1994 *J. Phys.: Condens. Matter* **6** 8795

[17] Moroni S, Conti S and Tosi M P 1996 *Phys. Rev.* B **53** 9688
[18] Gold A 1992 *Z. Phys.* B **89** 1
[19] Kim H K, Tao R and Wu F Y 1979 *Phys. Rev.* B **34** 7123
[20] Moudgil R K, Ahluwalia P K, Tankeshwar K and Pathak K N 1997 *Phys. Rev.* B **55** 544
[21] Mahan G D 1990 *Many-Particle Physics* (New York: Plenum)
[22] Kukkonen C A and Overhauser A W 1979 *Phys. Rev.* B **20** 550
See also Hedin L and Lundqvist B I 1971 *J. Phys. C: Solid State Phys.* **4** 2064
[23] Singwi K S and Tosi M P 1981 *Solid State Physics* vol 36 (New York: Academic) p 177
[24] Gold A 1997 *Z. Phys.* B **103** 491
[25] Gold A 1999 to be published
[26] Hoffmann G G and Pratt R P 1994 *Mol. Phys.* **82** 245